

# Locoregional Regulatory Peptide Receptor Targeting with the Diffusible Somatostatin Analogue $^{90}\text{Y}$ -Labeled DOTA<sup>0</sup>-D-Phe<sup>1</sup>-Tyr<sup>3</sup>-octreotide (DOTATOC): A Pilot Study in Human Gliomas<sup>1</sup>

Adrian Merlo,<sup>2</sup> Oliver Hausmann,  
Morten Wasner, Philipp Steiner, Andreas Otte,  
Eduard Jermann, Peter Freitag,  
Jean-Claude Reubi, Jan Müller-Brand,  
Otmar Gratzl, and Helmut R. Mäcke

Neurosurgical Clinic [A. M., O. H., M. W., O. G.], Institute and Clinic of Nuclear Medicine [A. O., J. M.-B.], Radiological Chemistry Unit [P. S., E. J., H. R. M.], and Neuroradiology [P. F.], University Hospital Basel, CH-4031 Basel, and Institute of Pathology, University of Berne, CH-3010 Berne [J.-C. R.], Switzerland

## ABSTRACT

Human gliomas, especially of low-grade type, have been shown to express high-affinity somatostatin receptor type 2 (J.-C. Reubi *et al.*, *Am. J. Pathol*, 134: 337–344, 1989). We enrolled seven low-grade and four anaplastic glioma patients in a pilot study using the diffusible peptidic vector  $^{90}\text{Y}$ -labeled DOTA<sup>0</sup>-D-Phe<sup>1</sup>-Tyr<sup>3</sup>-octreotide (DOTATOC) for receptor targeting. The radiopharmakon was locoregionally injected into a stereotactically inserted Port-a-cath. DOTATOC competes specifically with somatostatin binding to somatostatin receptor type 2 in the low nanomolar range as shown by a displacement curve of  $^{125}\text{I}$ -[Tyr<sup>3</sup>]-octreotide in tumor tissue sections. Diagnostic  $^{111}\text{In}$ -labeled DOTATOC-scintigraphy following local injection displayed homogeneous to nodular intratumoral vector distribution. The cumulative activity of regionally injected peptide-bound  $^{90}\text{Y}$  amounted to 370–3300 MBq, which is equivalent to an effective dose range between  $60 \pm 15$  and  $550 \pm 110$  Gy. Activity was injected in one to four fractions according to tumor volumes; 1110 MBq of  $^{90}\text{Y}$ -labeled DOTATOC was the maximum activity per single injection. We obtained six disease stabilizations and shrinking of a cystic low-grade astrocytoma component. The only toxicity observed was secondary perifocal edema. The activity:dose ratio (MBq:Gy)

represents a measure for the stability of peptide retention in receptor-positive tissue and might predict the clinical course. We conclude that SR-positive human gliomas, especially of low-grade type, can be successfully targeted by intratumoral injection of the metabolically stable small regulatory peptide DOTATOC.

## INTRODUCTION

Although aggressive management of glioblastoma multiforme can lead to a 2-year survival of up to 20%, long-term prognosis is grim (1, 2). In low-grade gliomas of WHO grade II, survival varies between the different subtypes. In ordinary astrocytomas, 5-year survival varies between 45 and 80% (3), and for oligodendrogliomas, prognosis is significantly better with a median survival of 9.8 years (4). Most gliomas are not curable by surgery, radiotherapy, or chemotherapy, and residual tumor of variable extent is left to adjuvant measures of limited efficacy (5).

The blood-brain barrier is a major obstacle for most antineoplastic agents. Therefore, direct intratumoral chemotherapy of gliomas has been tested, with limited success due to increased tissue clearance (6, 7). Direct intratumoral administration of radioimmunoconjugates (8, 9), toxin compounds (10), and gene-expressing viral vectors (11) can lead to high intratumoral doses or drug concentrations with reduced systemic toxicity. Vector distribution still might be limited and inhomogeneous. This drawback could be overcome by adapting a microinfusion technique that establishes a high convective flow in the extracellular space, leading to tumor responses within a range of 2–3 cm from the sites of injection using a transferrin-diphtheria toxin compound to treat brain tumors (10). Infiltrating glioma cell aggregates along distant white matter tracts might be difficult to reach using high molecular weight compounds. There is a need to develop smaller, highly diffusible vectors to target infiltrative disease. DOTATOC<sup>3</sup> can be regarded as a prototypical highly diffusible vector for regulatory peptide receptor targeting. We have already reported on the preliminary results of patients treated with  $^{90}\text{Y}$ -labeled DOTATOC for refractory neuroendocrine tumors (12). Here, we show that the  $^{111}\text{In}$ -labeled vector DOTATOC can readily penetrate large tumor volumes within 3–6 h after direct intratumoral injection, yielding a scintigraphic

Received 11/23/98; revised 1/25/99; accepted 2/1/99.

The costs of publication of this article were defrayed in part by the payment of page charges. This article must therefore be hereby marked *advertisement* in accordance with 18 U.S.C. Section 1734 solely to indicate this fact.

<sup>1</sup> This work was enabled by financial support from Regionale Krebsliga beider Basel (to A. M. and H. R. M.) and Grant 31-52969.97 from the Swiss National Science Foundation (to H. R. M.).

<sup>2</sup> To whom requests for reprints should be addressed, at Neurosurgical Clinic, University Hospital, Spitalstr. 21, CH-4031 Basel, Switzerland. Phone: 41-61-265-7120; Fax: 41-61-265-7138; E-mail: amerlo@uhbs.ch.

<sup>3</sup> The abbreviations used are: DOTATOC, DOTA<sup>0</sup>-D-Phe<sup>1</sup>-Tyr<sup>3</sup>-octreotide; MRI, magnetic resonance imaging; SR, somatostatin receptor; iRPT, interstitial radiolabeled peptide therapy; i.a., intraarterial; i.t., intratumoral.

Table 1 Clinical data, effective dose, activity:dose ratio, and response rates in [<sup>90</sup>Y]-labeled DOTATOC-treated glioma patients

Patient	Age, gender	Histology <sup>a</sup> location	Previous therapy	KPS <sup>b</sup>	Autoradiography <sup>c</sup>	Activity (fractions) (MBq)	Volume (ml)	Effective dose (Gy)	Activity:dose ratio (MBq/Gy)	Response <sup>d</sup>	Progression-free/Overall survival <sup>e</sup>
Low-grade gliomas (WHO grade II)											
TH	30, M	cAII-Rf	B-Dr-R*	90	ND	370 (2)	20	100 ± 20	3.7	CR	+4/+4
THi	31, M	AII-Rf	S	90	NA	555 (1)	15	380 ± 75	1.5	SD	+15/+15
CM	43, F	OII-Bf	B	100	ND	2405 (4)	36	550 ± 110	4.4	SD	18/18 <sup>f</sup>
BS	30, M	OII-Rf	S	100	++	555 (1)	12	208 ± 21	2.7	SD	+14/+14
AB	42, F	AII-Lf	B-R	100	ND	1100 (2)	30	280 ± 40	3.9	SD	+6/+6
BF	39, M	AII-Lf	B-R	60	ND	740 (3)	30	60 ± 15	12.3	sDet	0/8
NJ	43, M	AII-Lft	B-R	50	–	2200 (3)	79	99 ± 24	22.2	sDet	0/13
Anaplastic gliomas (WHO III-IV)											
FR	63, F	OIII-Rfp	S	100	++	1110 (2)	20	480 ± 55	2.3	SD	+10/+10
WH	43, M	GBM-Rto	S-R	100	+++	3330 (3)	130	335 ± 40	9.8	sDet	0/6
SI	37, F	GBM-Lt	S-R	80	–	2405 (4)	77	496 ± 100	4.8	SD	10/15
WP	28, M	GBM-Rto	S-R-C	90	ND	2035 (3)	47	147 ± 30	13.8	sDet	0/9

<sup>a</sup> c, cystic; AII, fibrillary astrocytoma; OII, oligodendroglioma grade II; AIII, anaplastic astrocytoma; GBM, glioblastoma multiforme; R, right; L, left; f, frontal; t, temporal; o, occipital; B, biopsy; R\*, brachytherapy with <sup>125</sup>I seeds; Dr, cyst drainage; R, external beam radiotherapy; S, surgery; C, chemotherapy.

<sup>b</sup> Karnofsky score at time of enrollment.

<sup>c</sup> ND, not done; NA, not assessable due to strong gliosis; +, SR-positive; –, SR-negative.

<sup>d</sup> CR, complete remission of a cyst in cystic AII; SD, stable disease = no progression on MRI and clinically stable for progression-free survival period as defined by a stable KPS and no signs of progression on MRI; PD, progressive disease; sDet, slow deterioration due to disease progression and possibly radionecrosis.

<sup>e</sup> Survival in months.

<sup>f</sup> Untreated epileptic status.

tumor image that closely resembles the lesion pattern on MRI. The rationale for using a somatostatin analogue to target human gliomas is founded in autoradiographic studies in which gliomas have been shown to express high affinity SR-2 (13). *In vitro* and *in vivo* animal studies have demonstrated that radiolabeled DOTATOC is a high-affinity ligand for SR-2 (14). Its uptake in receptor-expressing tissues and tumors could be inhibited by pretreating animals with 0.5 mg of octreotide (14, 15). The present study shows, for the first time in human brain tumors, that DOTATOC has high affinity binding to SR-2 in the low nanomolar range. We propose locoregional administration of <sup>90</sup>Y-labeled DOTATOC, iRPT, as a novel therapeutic form of diffusible brachytherapy to target SR-positive gliomas, especially of low-grade type.

## PATIENTS AND METHODS

**Patients.** The clinical data of 11 patients enrolled into this pilot study are shown in Table 1. Neutrophil and platelet counts, creatinine clearance, and prothrombin and partial thromboplastin times were required to be normal. All patients provided written informed consent. The protocol was approved by the Ethical Committee of the University Hospitals Basel. *In vivo* administration of radioconjugates had been authorized by the Federal Health Authorities.

**Radioconjugates.** We developed a new DOTA chelated somatostatin analogue, DOTATOC (DOTA: 1,4,7,10-tetraazacyclododecane-*N*, *N'*, *N''*, *N'''*-tetraacetic acid) in a five-step synthetic procedure according to GMP practice (16). <sup>111</sup>In-labeled DOTATOC was prepared as follows. Eight μg of

DOTATOC were dissolved in 190 μl of 0.4 M sodium acetate buffer (pH 5.5) with 7 mg of gentisic acid; after the addition of 6 mCi <sup>111</sup>InCl<sub>3</sub> (0.05 M HCl; Mallinckrodt Med., Petten, the Netherlands), the solution was heated at 90°C for 25 min. Quality control was obtained with the use of a Sep-Pak C<sub>18</sub> cartridge and high-performance liquid chromatography, resulting in highly pure radioligands with preserved receptor binding affinity ( $K_D = 2.2 \pm 0.5$  nM). The affinity of <sup>90</sup>Y-labeled DOTATOC was calculated from a competition assay to 1.8 ± 0.5 nM <sup>123</sup>I-labeled octreotide; the stability of <sup>90</sup>Y-labeled DOTATOC has been studied as described (16).

**Administration of Radiolabeled DOTATOC.** <sup>111</sup>In-labeled DOTATOC and <sup>90</sup>Y-labeled DOTATOC were directly injected into a Port-a-cath. Its capsule had been permanently implanted into the calvaria, and its catheter was inserted by stereotactic navigation (17). All patients were prepared with an i.v. bolus of dexamethasone (20 mg) and mannitol (20–40 g). After sterile puncture of the reservoir, the device was gently flushed with 1 ml of 1% human albumin, followed by injection of 1–1.5 ml of 111 MBq of <sup>111</sup>In-labeled DOTATOC and a defined activity of <sup>90</sup>Y-labeled DOTATOC within 60 s. Subsequently, the device was gently flushed with 2–3 ml of 1% human albumin. Eight to 12 mg of dexamethasone were administered daily for 3 weeks. In patients with a tumor volume >15 ml, 1–3 additional injections were administered in a 6-week interval.

**Scintigraphy and Biodistribution.** Planar scintigraphic images were obtained with a large-field-of-view camera (DIACAM; Siemens) as described (15, 17). In the first patient

**Table 2** Superior vector uptake after locoregional direct i.t. injection. Uptake ratios on cranial 24-h scintigrams after i.v., intracarotid (i.a.), and i.t. administration of [<sup>111</sup>In]-labeled DOTATOC<sup>a</sup> in a SR-positive heterogeneous glioblastoma multiforme displaying a low-grade oligodendroglioma component

Injection	$K/T^b$	$T/B_{\text{head}}$	$T/B_{\text{abd}}$	$K/B_{\text{abd}}$
i.v.	29.40	0.65	0.43	12.60
i.a.	26.41	0.80	0.55	14.66
i.t.	0.03	18.31	61.25	1.58

<sup>a</sup> 100–190 MBq.

<sup>b</sup>  $K$ , kidney;  $T$ , tumor;  $B_{\text{head}}$ , cephalic background;  $B_{\text{abd}}$ , abdominal background.

(W. P.), three different routes of injection were serially performed to compare tumor uptake following i.v., i.a. (into the right proximal internal carotid), and direct i.t. injection into the Port-a-cath capsule (Table 2). Images were acquired 30 min and 1, 2, 5, 24, 48, and 72 h after systemic and locoregional injections of 190 MBq (i.v. and i.a.) and of 100 MBq (i.t.) <sup>111</sup>In-labeled DOTATOC. The uptake (counts/pixel) was determined in specific regions of interest of the cephalic and the abdominal spine background, of the kidneys and the tumor cavity 24 h postinjection. Subsequently, uptake ratios of kidney over tumor [ $K/T$ ], of tumor over cephalic background [ $T/B_{\text{head}}$ ], of tumor over abdominal spine background [ $T/B_{\text{abd}}$ ], and of kidney over abdominal spine background [ $K/B_{\text{abd}}$ ] were determined. Radioactivity was measured in blood and urine over 72 h. The chemical structure of the radioligand in blood and urine was determined by high-performance liquid chromatography. In all of the other patients, the radiopharmakon was injected locoregionally because uptake proved to be far superior after locoregional injection as compared with systemic application (Table 2). In these patients, cranial and abdominal scintigrams were obtained daily for 5 days.

**Autoradiography.** Surgical specimens were immediately frozen in liquid nitrogen after resection. Frozen material was cut on a cryostat for autoradiographic visualization of SRs using the stable octapeptide, <sup>125</sup>I-[Tyr<sup>3</sup>]-octreotide. The ligand is iodinated and purified as described previously and characterized in standard binding assays (13, 18), using a 2-h incubation period at ambient temperature in the presence of 30,000 dpm/100  $\mu$ l of <sup>125</sup>I-[Tyr<sup>3</sup>]-octreotide. A tumor is considered receptor positive on an autoradiogram if at least part of it has an absorbance value for the total binding at least twice the value measured for the nonspecific binding. Care was taken to identify admixture of normal brain next to tumor tissue.

**Volumetry.** The tumor volumes were analyzed by defining the tumor extensions of each patient on the T1-weighted gadolinium-DOTA enhanced MR images that were acquired prior to iRPT. Each tumor was manually outlined on digitized image data using the NIH Image software. Volumes were calculated by multiplying the tumor area of each slice with slice thickness corrected by an interslice gap factor on Excel Sheet software.

**Dosimetry.** The doses delivered to the neoplasm and to normal tissues were calculated applying both Medical International Radiation Dosimetry and Monte Carlo formalism (19, 20). Uptake was defined as the ratio  $IA:IA_0$  of the integral over

the absorbed activity  $IA$  to the integral over the injected activity  $IA_0$ . The value of these integrals depends upon the physical ( $t_{1/2 \text{ phys}}$ ) and biological ( $t_{1/2 \text{ biol}}$ ) half-lives of the peptidic vector DOTATOC. The effective half-life ( $t_{1/2 \text{ eff}}$ ) is relevant for the calculation of the accumulated dose  $D$ , using the formula  $t_{1/2 \text{ eff}} = (t_{1/2 \text{ phys}} \times t_{1/2 \text{ biol}})/(t_{1/2 \text{ phys}} + t_{1/2 \text{ biol}})$ . Within the first 24 h after locoregional injection,  $t_{1/2 \text{ eff}}$  is strongly influenced by biodistributive processes. Thereafter,  $t_{1/2 \text{ eff}}$  is equivalent to  $t_{1/2 \text{ phys}}$ . Secondary re-uptake of peptidic vectors after tissue clearance after intratumoral injection is insignificant, because the amount of reabsorbed peptides is negligible in comparison with the specifically bound vectors after primary injection. Uptakes of around 50% are generally obtained after i.t. injection of DOTATOC, which is about 2 log scales better compared with systemic injection. The error  $E$  in the estimated dose is related to the uncertainty  $\Delta U$  in the uptake as  $E = \Delta U/U$ . Distinct from systemic therapy where a phantom has to be used (11), the activity  $A_0$  at the time of injection  $t_0$  can be used for calibration. The uptake as measured by planar scintigraphy in anterior and lateral projections yields consistent values over time in the range of  $\pm 10\%$ , irrespective of tumor volume and shape. For i.t. injection of <sup>90</sup>Y-labeled DOTATOC with an average uptake of  $50 \pm 10\%$ , an uncertainty of 20% results for the estimated therapeutic dose.

## RESULTS

**Patients.** Patients having seven low-grade gliomas and four anaplastic gliomas, which have been histologically classified according to the WHO grading system (21), were enrolled into this pilot study after having signed the informed consent form as requested by the Ethical Committee of the University Hospital Basel (Basel, Switzerland). The clinical data are summarized in Table 1. These patients showed disease progression despite previous surgery, external beam radiotherapy (55–60 Gy), brachytherapy with <sup>125</sup>I seeds, and/or chemotherapy [1-(2-chloroethyl)-3-cyclohexyl-1-nitrosourea], developing signs of increased intracranial pressure due to volumetric expansion of solid tumor or associated cystic components. Tumor progression was confirmed by tissue sampling during biopsy and/or re-craniotomy.

**Stability and <sup>90</sup>Y Release of DOTATOC.** The vector is a small ( $M_r$  1400) and stable regulatory peptidic analogue of somatostatin conjugated to the radiometal chelator DOTA creating DOTA<sup>0</sup>-D-Phe<sup>1</sup>-Tyr<sup>3</sup>-octreotide, which we dubbed DOTATOC (14). In contrast to DTPA<sup>0</sup>-D-Phe<sup>1</sup>-octreotide (OctreoScan), DOTATOC allows stable labeling with <sup>90</sup>Y, a  $\beta^-$  emitter suitable for therapy (maximum  $\beta^-$  energy, 2.3 MeV; half-life, 64 h; range, 2–5 mm). The stability of the tracer DOTATOC was excellent when studied under physiological conditions. In PBS (37°C), no release of <sup>90</sup>Y was seen over >5 days, a critical prerequisite for safe *in vivo* application. Moreover, the half-life in human serum was determined to be around 2300 h ( $t_{1/2}$  of <sup>90</sup>Y, 64 h; Ref. 16). This high stability is most likely due to a very efficient encapsulation of the radiometal <sup>90</sup>Y inside the cavity which is formed by the chelator DOTA.

**Receptor Autoradiography and Binding Specificity of DOTATOC.** In six cases undergoing tumor debulking by craniotomy, frozen tumor samples could be obtained to deter-

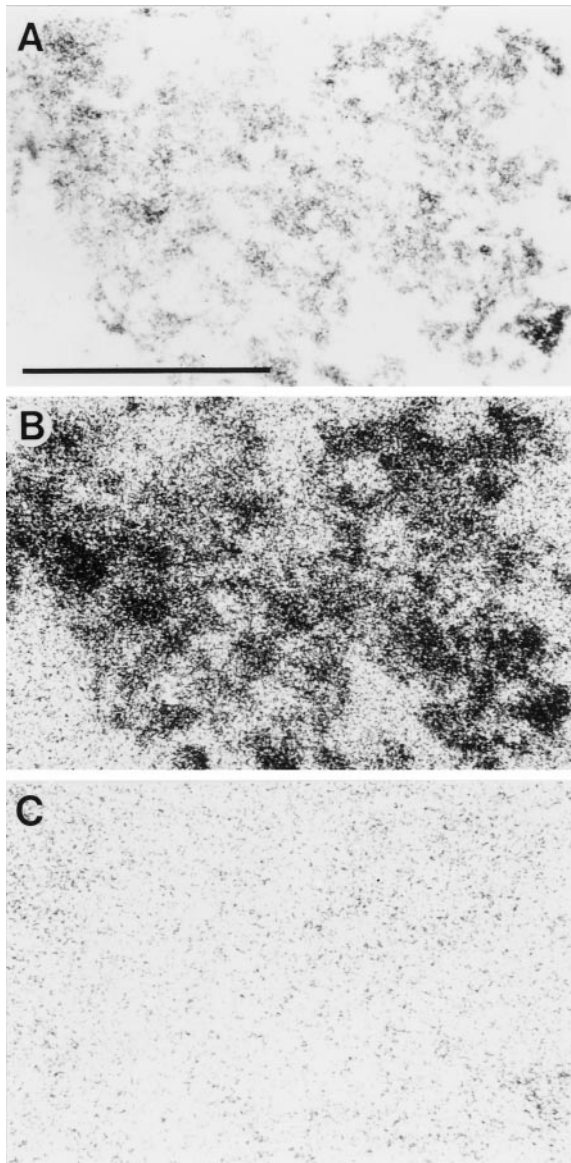


Fig. 1 *In vitro* somatostatin autoradiography showing SRs in oligodendroglioma BS (Table 1). A, H&E-stained section. Bar, 1 mm. B, autoradiogram showing total binding of  $^{125}\text{I}$ -[Tyr<sup>3</sup>]-octreotide. The entire tumor is labeled. C, autoradiogram showing nonspecific binding of  $^{125}\text{I}$ -[Tyr<sup>3</sup>]-octreotide (in the presence of  $10^{-6}$  M octreotide).

mine the somatostatin receptor status; tissue acquired during stereotactic sampling was not sufficient for SR analysis in the residual five cases. Because prior brachytherapy, tumor tissue was not assessable in case THi (Table 1). In case BS, high SR density and high affinity binding of the SR for octreotide and for DOTATOC was detected by *in vitro* receptor autoradiography (Figs. 1 and 2), whereas the control peptide SS-28 does not show binding. A similar finding was obtained in an anaplastic oligodendroglioma (case FR, data not shown). One glioblastoma that grew out of an astrocytoma grade III (case WH) displayed an exceptionally high receptor density, despite the malignant phenotype. In the other two assessable cases (NJ and SI), the

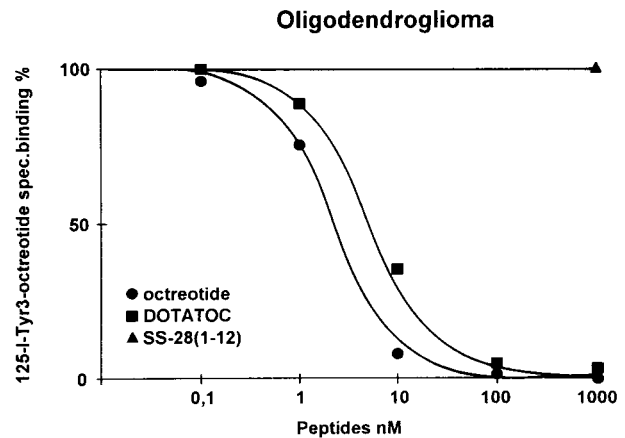


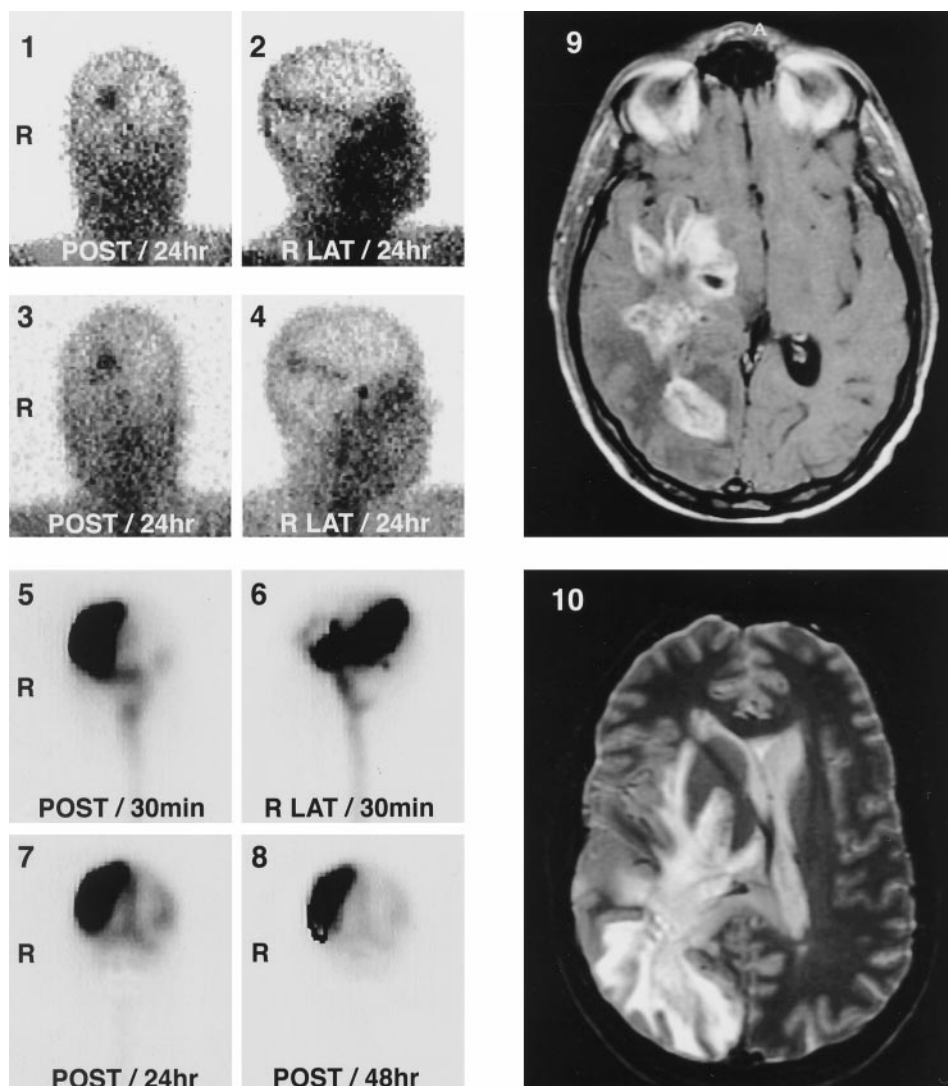
Fig. 2 Displacement curve of  $^{125}\text{I}$ -[Tyr<sup>3</sup>]-octreotide in tissue sections from oligodendroglioma BS (Table 1). Sections were incubated with 30,000 dpm/100  $\mu\text{l}$  of  $^{125}\text{I}$ -[Tyr<sup>3</sup>]-octreotide and increasing concentrations of unlabeled octreotide (●), DOTATOC (■), or 1000 nM SS-28 (1–12) (▲).

surgically selected specimens were SR negative. In case SI, *in vivo* receptor density appeared to be high as estimated by the activity:dose ratio (see below), suggesting sampling error due to inhomogeneous SR-2 distribution or loss of assessability during tissue processing.

**Tumor Uptake after Systemic and Intratumoral Injection.** In the first patient (WP), we compared direct i.a. (proximal internal carotid) injection of  $^{111}\text{In}$ -labeled DOTATOC to i.v. injection and direct intratumoral injection. The various uptake ratios are shown in Table 2. For each value, counts/pixel were calculated 24 h after injection, when the effective  $t_{1/2}$  approximates the physical  $t_{1/2}$  (see below). Intratumoral application of  $^{111}\text{In}$ -labeled DOTATOC showed improved biodistribution, background clearance, and renal accumulation as compared with systemic administration. We did not observe a “first pass effect” because uptake ratios did not differ significantly after i.v. and i.a. injections. After systemic injection, radioactivity clears quickly from the blood, according to a two-exponential curve ( $\alpha$ ,  $\beta$ ) with  $t_{1/2}$  ( $\alpha$ ) =  $5 \pm 1$  min (76% radioactivity) and  $t_{1/2}$  ( $\beta$ ) =  $110 \pm 30$  min (24% radioactivity; Ref. 15), which was confirmed in the i.v. and i.a. injection protocol of patient WP. The radiolabeled peptide is highly stable. Radioactivity from systemic circulation is mainly excreted via the kidneys and found intact in the urine within the first 4 h (>96% intact, >50% of activity in the urine). Thereafter, two metabolites are detected at low concentrations in the urine, the main one being  $^{111}\text{In}$ -labeled DOTA-D-Phe<sup>1</sup> (15).

**Biodistribution of DOTATOC after Intratumoral Injection.** Direct intratumoral injection of drugs into gliomas bypasses the blood-brain barrier and allowed us to increase tumor dose while reducing systemic toxicity. However, rapid tissue clearance into systemic circulation was observed after intratumoral administration of chemotherapeutic agents (6, 7). This problem can be overcome by using ligands that specifically bind to receptors expressed by tumor cells, as shown here by using the SR-2-DOTATOC system. Within 3–6 h after local injection, extensive vector distribution throughout the entire

**Fig. 3** Tumor uptake of  $^{111}\text{In}$ -labeled DOTATOC (images 1–8) and MRI tumor extension (images 9 and 10) in glioblastoma of case WP. In this first patient, cranial scintigrams were obtained following i.v. (images 1 and 2), i.a. (images 3 and 4), and i.t. (images 5–8) injections at time points as denoted. Axial gadolinium-enhanced T1- and T2-weighted MRI section of the brain show large tumor mass. Despite a favorable diffusion pattern, this patient was not likely to benefit from iRPT because the activity:dose ratio of 13.8 MBq/Gy is indicative of low level expression of SR-2. Repeat stereotactic biopsy proved tumor heterogeneity because areas of low-grade oligodendrocytic differentiation were disclosed in this so called “*de novo* glioblastoma.”



tumor mass was observed on cranial scintigrams, yielding a stable image for up to 12 days (Fig. 3, images 1–8; Fig. 4, images 1–6).  $^{111}\text{In}$ -labeled DOTATOC distribution was confined to radiological tumor borders, giving rise to homogeneous as well as nodular patterns on cranial scintigrams, and diffusion has been observed across the neoplastically infiltrated corpus callosum into the affected contralateral frontal lobe (Fig. 4, images 3 and 5). We could not detect diffusion into adjacent normal brain areas on planar cranial scintigrams. About 50% of the locally injected activity is bound by SR-positive tumors, and a similar amount of activity diffuses into systemic circulation within 24 h. Thereafter, the effective and the physical half-lives of  $^{111}\text{In}$  ( $t_{1/2} = 67.4$  h) or  $^{90}\text{Y}$  ( $t_{1/2} = 64$  h), respectively, became virtually identical because activity in serum and urine approached zero as shown in an illustrative example (Fig. 5). This is indicative of a prolonged local effect after specific receptor-ligand interaction.

**Targeting SR-positive Gliomas with  $^{90}\text{Y}$ -labeled DOTATOC.** Eleven glioma patients were enrolled into this pilot study and received one to four fractions of exclusively locally injected  $^{90}\text{Y}$ -labeled DOTATOC. In cases with a tumor volume  $>15$  ml, one to three injections were repeated in 6-week intervals. The activity of  $^{90}\text{Y}$ -labeled DOTATOC per single injection ranged between 185 and 1100 MBq (5–30 mCi), and total cumulative activity per patient between 370 MBq (10 mCi) and 3330 MBq (90 mCi). Patients were dismissed 1–2 days after local injection under an antiedematous regimen for 3 weeks to prevent secondary radiogenic edema.

In patient BS, a single injection of 555 MBq  $^{90}\text{Y}$ -labeled DOTATOC (effective dose,  $208 \pm 21$  Gy) resulted in an activity:dose ratio of 2.7 MBq/Gy (Table 1). This low ratio is indicative for high *in vivo* SR expression and specific binding of DOTATOC to SR, corresponding with the high density of SR-2 receptors by autoradiography (Fig. 1) and a displacement curve (Fig. 2) on tissue sections of this patient.

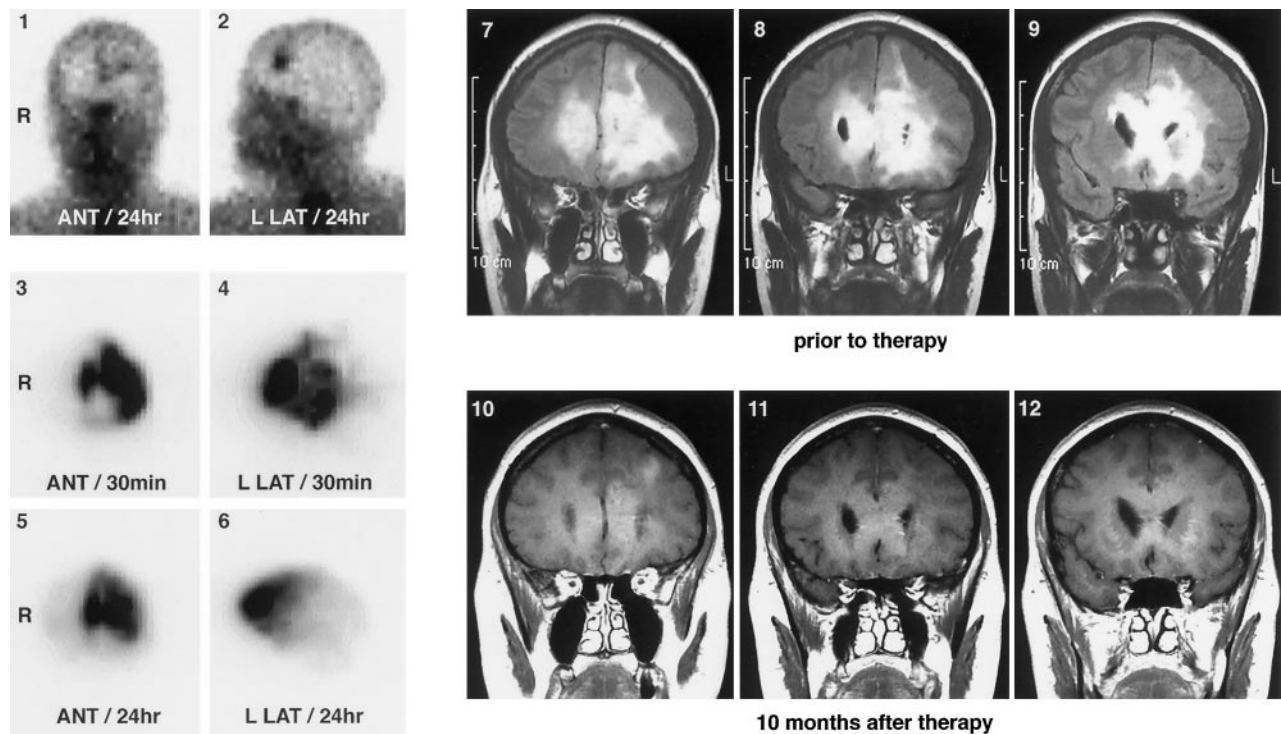


Fig. 4 Tumor uptake of  $^{111}\text{In}$ -labeled DOTATOC (images 1–6) and marked reduction of perifocal enhancement after  $^{90}\text{Y}$ -labeled DOTATOC treatment (images 7–12) in oligodendroglioma patient CM (Table 1). The cranial scintigram after i.v. (images 1 and 2) injection is shown as compared with direct intratumoral (images 3–6) stereotactically guided administration at denoted time points. Coronal gadolinium-enhanced, T1-weighted MRI prior to (images 7–9) and after (images 10–12) local injection of 2405 MBq of  $^{90}\text{Y}$ -labeled DOTATOC shows complete vanishing of perifocal edema. The effective dose was  $550 \pm 110$  Gy, and the activity:dose ratio was 4.4 MBq/Gy. Steroid medication had been stopped 4 months before the control MRI.

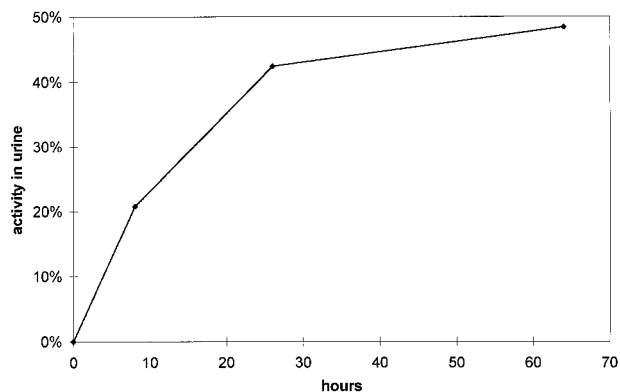


Fig. 5 Activity recovered from urine as percentage of total injected activity of  $^{90}\text{Y}$ -labeled DOTATOC in a representative sample (case TH). *Bremsstrahlung* was measured during 64 h after direct injection of 185 MBq of  $^{90}\text{Y}$ -labeled DOTATOC into a cystic fibrillary low-grade astrocytoma grade II. The effective half-life approximates the physical  $t_{1/2}$  24 h after injection.

In patient CM suffering from a large bifrontal oligodendroglioma that extended into the genu corporis callosi,  $^{90}\text{Y}$ -labeled DOTATOC induced a partial response as shown on follow-up MRIs 4 and 10 months after initiating iRPT (Fig. 4, images 7–12). Diffusion of the peptidic vector from the left

frontal lobe across the corpus callosum to the contralateral site is clearly visible in Fig. 4 (images 3 and 5). The cumulative locally injected activity in this case amounted to 2405 MBq, which translates into an effective dose of  $550 \pm 110$  Gy, yielding a low activity:dose ratio of 4.4 MBq/Gy. This dose has been well tolerated without any signs of early or intermediate toxicity (observation interval, 18 months). The nearly complete vanishing of the contrast-enhancing perifocal volume on the follow-up MRIs is not caused by a general reduction of contrast enhancement that occurs as a result of steroid therapy, which had been discontinued by the time of control MRIs. The remaining low-grade patients are summarized in Table 1.

We also tested the SR-2 DOTATOC approach in four anaplastic gliomas (WHO III–IV). It is of note that most glioblastomas cannot satisfactorily be targeted with DOTATOC because malignancy grade is inversely correlated to levels of SR-2 expression (13). Even if an exceptionally high content of SR-2 is found by autoradiography as in the case of WH (glioblastoma multiforme progressing from an astrocytoma grade III), the elevated activity:dose ratio suggests inhomogeneous SR-2 distribution or lack of SR-2 expression in the infiltrating clonal cell population. The observation in this patient that the dose continuously dropped from the first to to the third local injection of 1100 MBq  $^{90}\text{Y}$ -labeled DOTATOC from  $145 \pm 28$  Gy to  $60 \pm 12$  Gy would argue for a gradual loss of SR-2 during progression. In patient WP (Tables 1 and 2; Fig. 3), a glioblastoma that

progressively grew within the patient's right hemisphere was attacked with a total activity of 2035 MBq, resulting in an effective dose of  $147 \pm 30$  Gy. In this case, inhomogeneous tissue composition was proven histologically (glioblastoma with areas of low-grade oligodendrocytic differentiation). The high activity:dose ratio of 13.8 MBq/Gy is concordant with lack of response. The glioblastoma in patient SI (Table 1) was locally treated with a total activity of 2405 MBq  $^{90}\text{Y}$ -labeled DOTATOC (effective dose,  $496 \pm 100$  Gy), stabilizing the disease for 10 months. The favorable activity:dose ratio of 4.8 MBq/Gy suggests at least initially the presence of SR in certain tumor areas, although a resected specimen from the temporal tumor margin was negative by *in vitro* autoradiography, most likely due to a sampling error. This example points to the limits of *in vitro* autoradiography with regard to inhomogeneous receptor expression and tissue differentiation in gliomas. The activity:dose ratio appears to be a more reliable measure for dose and response estimates.

**Tumor Dosimetry.** In case TH, dosimetry was established by two independent methods. In the first approach, serial scintigrams alone were used to obtain a dose estimate, whereas in the second approach, the integrated activity of the urine over the first 48 h after intracystic injection was measured, as shown for a representative example in Fig. 5. The first approach was adopted for all other patients. The small fraction ( $<10\%$ ) of the activity deposited in the kidneys and in the spleen was taken into account in both approaches. Given the average  $\beta$  energy of 0.9 MeV release per decay of an  $^{90}\text{Y}$  atom and an estimated average range of 3 mm of tissue, a total dose of  $\sim 100$  Gy was deposited over a 5-mm thick layer of cyst surface (volume 30 ml, daily production  $\pm 2$  ml). The activity:dose ratio in this case was 3.7 MBq/Gy.

Within the first 24 h after locoregional injection,  $t_{1/2 \text{ eff}}$  is strongly influenced by biodistributive processes. Thereafter,  $t_{1/2 \text{ eff}}$  is equivalent to  $t_{1/2 \text{ phys}}$ . Secondary reuptake of peptidic vectors after tissue clearance after intratumoral injection is insignificant, because the amount of reabsorbed peptides is negligible in comparison with the specifically bound vectors following primary injection. Uptakes of around 50% are generally obtained after intratumoral injection of DOTATOC, which is about 2 log scales better compared with systemic injection. The error  $E$  in the estimated dose is related to the uncertainty  $\Delta U$  in the uptake as  $E = \Delta U/U$ .

**High Activity:Dose Ratio and Disease Progression in Low-Grade Gliomas.** High activity:dose ratios of 12.3 and 22.2, respectively, were obtained in patients BF and NJ, despite the generally more favorable histology of fibrillary astrocytoma WHO grade II (Table 1), suggesting low expression of SR-2. Intratumoral vector distribution was found to be inhomogeneous, the radiopeptide cleared rapidly from the tumor compartment, and receptor autoradiography displayed absence of SR in the one tumor sample tested (patient NJ, data not shown). The activity:dose-ratio is an *in vivo* measure for peptide retention by stable long-term binding of receptor-positive tissue. Because dose is calculated by energy/volume, favorable low ratios can only be obtained if SR-2 distribution throughout the tumor mass is relatively homogeneous. SR-2 expression can be considered to be a differentiation marker, and the activity:dose ratio might

become a useful tool for dose estimates prior to therapy and a prognostic marker in low-grade gliomas.

**Toxicity.** Radiogenic edema represented the only side effect attributable to this local radiopeptide therapy. We did not observe hematological, chemical, endocrinological, or renal toxicity during the follow-up period (Table 1). Seizure activity did not increase in frequency as a consequence of this therapy. Clinical deterioration was considered to be mainly due to tumor progression based on tumor distribution patterns on MRI; however, in one case (SI), radiation necrosis plus neoplastic tissue was detected histologically during a follow-up biopsy 11 months after initiation of iRPT (SI). It is of note that in a parallel ongoing clinical Phase I study using  $^{90}\text{Y}$ -labeled DOTATOC to treat end-stage carcinoids by i.v. injections, renal toxicity has only been observed at an cumulative activity of  $>7500$  MBq/m<sup>2</sup> ( $>200$  mCi/m<sup>2</sup>).

## DISCUSSION

Theoretically, four major criteria have to be met for the successful establishment of biologically guided radiotherapy protocols of primary brain tumors: (a) high and frequent expression of tumor-associated markers as biological targets; (b) the availability of high-affinity diffusible targeting agents that reach all distant sites of tumor cell infiltration; (c) efficient radionuclide labeling of the targeting agents, *i.e.*, preservation of the binding properties and *in vivo* stability of the radioconjugate yielding long residence time on targeted tumor cells; and (e) a radionuclide energy profile that destroys tumor cells in oxygenated and hypoxic areas without dissipating potentially harmful energy into adjacent normal brain areas. Under ideal conditions, targeting SR-2 by DOTATOC fulfills these four criteria, thus representing a prototype system to develop and establish radiopeptide therapy for brain tumors. It has been shown previously that predominantly differentiated gliomas express intermediate to high levels of SR-2 (13). In this study, we found binding of DOTATOC to SR-2 to be specific in the low nanomolar range as shown by *in vitro* autoradiography (Fig. 1) and by a displacement curve (Fig. 2). Uptake of the vector  $^{90}\text{Y}$ -labeled DOTATOC could be substantially improved by direct i.t. locoregional injection as compared with the very limited tumor uptake after i.v. or intraarterial application. As for F(ab')<sub>2</sub> fragments (22), we could not observe an improved uptake of the peptidic vector after direct i.a. (proximal internal carotid) injection as compared with i.v. administration. The prolonged vector retention is very likely to be a consequence of specific receptor binding and internalization of the receptor-ligand complex.

In this pilot study, six disease stabilizations and shrinkage of a cystic low-grade astrocytoma component were obtained using this iRPT protocol (Table 1). Patients were evaluated based on neuroradiological criteria and progression-free survival. In low-grade gliomas, responses appear to directly correlate with a given tumor's SR status, as calculated by the activity:dose ratio (MBq/Gy) that can be regarded as a quantitative *in vivo* measure for peptide binding. Patients with a ratio  $\gg 5$  MBq/Gy are not very likely to benefit from this approach (Table 1). We observed a trend toward longer progression-free survival in low-grade glioma patients with an activity:dose-ratio  $< 5$ . Whether this ratio really is an independent prognostic factor

remains to be shown in a controlled clinical trial. In anaplastic gliomas, especially glioblastomas, the situation is more complex; decreased expression of SR receptors during tumor progression potentially confounds the interpretation of autoradiographic receptor assays by sampling error as suspected for cases SI and WH (Table 1). In these cases, the activity:dose ratio appears to be more robust to predict a response to this form of radiopeptide therapy than autoradiography alone. A slight volume effect was observed in a large bifrontal oligodendroglioma after fractionated intratumoral administration of an effective dose of  $550 \pm 110$  Gy of  $^{90}\text{Y}$ -labeled DOTATOC; perifocal enhancement completely disappeared, allowing cessation of steroids (Fig. 4), and tumor volumetry showed a reduction by  $\pm 10\%$ . A modest effect on tumor volumes has also been observed in systemically treated tumors of the neuroendocrine system using  $^{90}\text{Y}$ -labeled DOTATOC (12). It is known from external beam radiotherapy of low-grade gliomas, pituitary adenomas and meningiomas that residual tumor can persist for many years while growth is arrested (23, 24).

In the central nervous system, somatostatin acts as a neurotransmitter in the hypothalamo-hypophyseal axis, the hippocampus, the cerebral cortex, and the brainstem (25). Nevertheless, normal tumor-surrounding brain tissue does not display peptide uptake after systemic administration of radiolabeled peptides because of the preservation of the blood-brain barrier. The pituitary, which is located outside this barrier, is usually visible after i.v. or i.a. injection of  $^{111}\text{In}$ -labeled DOTATOC (Ref. 26 and Fig. 3, images 2 and 4). After stereotactically guided i.t. injection, we could not observe diffusion of vector into adjacent normal brain areas, which might be due to the limited resolution of scintigraphy because convective forces are expected to facilitate vector distribution along elevated i.t. pressure gradients from the tumor center toward the periphery into normal brain tissue (27). Loss of peptides from the i.t. compartment into systemic circulation across the disturbed blood-brain barrier competes with this convective interstitial transport mechanism. Another critical factor that might explain this i.t. distribution pattern is the size of the extracellular space, which can be as large as 20–40% of a given tissue volume in gliomas as compared with 6–7% in normal brain (28). High-affinity binding followed by receptor-ligand internalization might best explain the long i.t. residence times of DOTATOC for 2 weeks observed in these patients.

What was the maximum tolerated dose following intratumoral administration of  $^{90}\text{Y}$ -labeled DOTATOC in this study? Because of radiogenic brain edema requiring antiedematous therapy, we limited the maximum activity applied in a single intratumoral injection to 1110 MBq of  $^{90}\text{Y}$ -labeled DOTATOC. We administered total cumulative activities up to 3330 MBq, resulting in effective doses up to 550 Gy. Even higher dose ranges (60–1300 Gy) have been administered for intracavitary injection of  $^{131}\text{I}$ -labeled anti-tenascin antibodies to treat cystic glioblastomas; dose-limiting neurological and hematological toxicities have been reported to occur at an activity of 4400 MBq (29).

In conclusion, targeting SRs with locoregionally administered  $^{90}\text{Y}$ -labeled DOTATOC has the potential to become a therapeutic option for SR-positive solid and cystic gliomas, especially of low-grade type. In a future controlled trial, it will

be mandatory to monitor residual tumor during therapy, for instance by positron emission tomography using the positron emission tomography-tracer  $^{86}\text{Y}$ . For most glioblastomas displaying reduced expression of SR, more specific receptor-ligand systems need to be developed.

## ACKNOWLEDGMENTS

We are thankful for the medical, nursing, and technical support that we received from S. Albrecht, T. Böhler, I. Goetze, D. Kouao-Bile, U. Läderach, B. Leu, P. Powell, B. Schultz, L. Schwob, B. Waser, and T. Zajic.

## REFERENCES

- Black, P. M. Brain Tumors. *N. Engl. J. Med.*, 324: 1555–1564, 1991.
- Berger, M. S., Leibel, S. A., Briner, J. A., Finlay, J. L., and Levin, V. A. Primary central nervous system tumors of the supratentorial compartment. *In: Levin V. A. (ed.), Cancer in the Nervous System*, pp. 57–126, New York: Churchill Livingstone, 1995.
- Shaw, E. G., Scheithauer, B. W., and O'Fallon, J. R. Management of supratentorial low-grade gliomas. *Semin. Radiat. Oncol.*, 1: 23–31, 1991.
- Shaw, E. G., Scheithauer, B. W., O'Fallon, J. R., Tazelaar, H. D., and Dudley, H. D. Oligodendrogliomas: The Mayo Clinic experience. *J. Neurosurg.*, 76: 428–434, 1992.
- Walker, M. D., Green, S. B., Byar, D. P., Alexander, E., Batzdorf, U., Brooks, W. H., Hunt, W. E., MacCarty, C. S., Mahaley, M. S., Mealey, J., Owens, G., Ransohoff, J., Robertson, J. T., Shapiro, W. R., Smith, K. R., Wilson, C. B., and Strike, T. A. Randomized comparisons of radiotherapy and nitrosoureas for the treatment of malignant glioma after surgery. *N. Engl. J. Med.*, 303: 1323–1329, 1980.
- Garfield, J., Dayan, A. D., and Weller, R. O. Postoperative intracavitary chemotherapy of malignant supratentorial astrocytomas using BCNU. *Clin. Oncol.*, 1: 213–222, 1975.
- Brem, H., Piantadosi, S., Burger, P. C., Walker, M., Selker, M., Vick, N. A., Black, K., Sisti, M., Brem, S., and Mohr, G. Placebo-controlled trial of safety and efficacy of intraoperative controlled delivery by biodegradable polymers of chemotherapy for recurrent gliomas. *Lancet*, 345: 1008–1012, 1995.
- Riva, P., Arista, A., Franceschi, G., Frattarelli, M., Sturiale, C., Riva, N., Casi, M., and Rossitti, R. Local treatment of malignant gliomas by direct infusion of specific monoclonal antibodies labeled with  $^{131}\text{I}$ : comparison of the results obtained in recurrent and newly diagnosed tumors. *Cancer Res.*, 55: 5952s–5956s, 1995.
- Papanastassiou, V., Pizer, B. L., Coakham, H. B., Bullimore, J., Zananiri, T., and Kemshead, J. T. Treatment of recurrent and cystic malignant glioma by a single intracavitary injection of I-131 monoclonal antibody: feasibility, pharmacokinetics and dosimetry. *Br. J. Cancer*, 67: 144–151, 1993.
- Laske, D. W., Youle, R. J., and Oldfield, E. H. Tumor regression with regional distribution of the targeted toxin TF-CRM107 in patients with malignant brain tumors. *Nat. Med.*, 3: 1362–1368, 1997.
- Ram, Z., Culver, K. W., Oshiro, E. M., Viola, J. L., DeVroom, H. L., Otto, E., Long, Z., Chiang, Y., McGarrity, G. J., Muul, L. M., Katz, D., Blaese, R. M., and Oldfield, E. H. Therapy of malignant brain tumors by intratumoral implantation of retroviral vector-producing cells. *Nat. Med.*, 3: 1354–1361, 1997.
- Otte, A., Mueller-Brand, J., Dellas, S., Nitzsche, E. U., Herrmann, R., and Maecke, H. R. Yttrium-90-labelled somatostatin analogue for cancer treatment. *Lancet*, 351: 417–418, 1998.
- Reubi, J. C., Horisberger, U., Lang, W., Koper, J. W., Braakman, R., and Lamberts, S. W. J. Coincidence of EGF receptors and somatostatin receptors in meningiomas but inverse, differentiation dependent relationship in glial tumors. *Am. J. Pathol.*, 134: 337–344, 1989.
- deJong, M., Bakker, W. H., Krenning, E. P., Breeman, W. A. P., van der Pluijme, M. E., Bernard, B. F., Visser, T. J., Jermann, E., Béhé, M., Powell, P., and Mäcke, H. R. Yttrium-90 and indium-111 labeling,



- receptor binding and biodistribution of [DOTA<sup>0</sup>, D-Phe<sup>1</sup>, Tyr<sup>3</sup>]octreotide, a promising somatostatin analogue for radionuclide therapy. *Eur. J. Nucl. Med.*, *24*: 368–371, 1997.
15. Otte, A., Jermann, E., Béhé, M., Götze, M., Bucher, H. C., Roser, H. W., Heppeler, A., Müller-Brand, J., and Mäcke, H. R. DOTATOC: a powerful new tool for receptor-mediated radionuclide therapy. *Eur. J. Nucl. Med.*, *24*: 792–795, 1997.
16. Ruser, G., Ritter, W., and Maecke, H. R. Synthesis and evaluation of two new bifunctional carboxymethylated tetraazamacrocyclic chelating agents for protein labeling with indium-111. *Bioconj. Chem.*, *1*: 345–349, 1990.
17. Merlo, A., Jermann, E., Hausmann, O., Chiquet-Ehrismann, R., Probst, A., Landolt, H., Mäcke, H. R., Müller-Brand, J., and Gratzl, O. Biodistribution of <sup>111</sup>In-labelled SCN-BZ-DTPA-BC-2 MAB following locoregional injection into glioblastomas. *Int. J. Cancer*, *71*: 810–816, 1997.
18. Reubi, J. C., Probst, A., Cortès, R., and Palacios, J. M. Distinct topographical localisation of two somatostatin receptor subpopulations in the human cortex. *Brain Res.*, *406*: 391–396, 1987.
19. MIRDPamphlet, No. 11. New York: Society of Nuclear Medicine, 1985.
20. Loevinger, R., and Berman, M. A schema for absorbed dose calculation for biologically distributed radionuclides. MIRDPamphlet No. 1. *J. Nucl. Med.*, *9* (Suppl. 1): 7–14, 1968.
21. Kleihues, P., Burger, P. C., and Scheithauer, B. W. Histological typing of tumours of the Central Nervous System. WHO International Histological Classification of Tumours. Berlin: Springer, 1993.
22. Zalutsky, M. R., Moseley, R. P., Benjamin, J. C., Colapinto, E. V., Fuller, G. N., Coakham, H. P., and Bigner, D. D. Monoclonal antibody and F(ab')<sub>2</sub> fragment delivery to tumor in patients with glioma: comparison of intracarotid and intravenous administration. *Cancer Res.*, *50*: 4105–4110, 1990.
23. Fisher, J. B., Bauman, G. S., Leighton, C. E., Stitt, L., Cairncross, J. G., and Macdonald, D. R. Low-grade glioma in children: tumor volume response to radiation. *J. Neurosurg.*, *88*: 969–974, 1998.
24. Goldsmith, B. J., Wara, W. M., and Wilson, C. B. Postoperative irradiation for subtotally resected meningiomas. *J. Neurosurg.*, *80*: 195–201, 1994.
25. Krenning, E. P., Kweskeboom, D. J., Pauwels, S., Kvols, L. K., and Reubi, J. C. Somatostatin receptor scintigraphy. *In*: L. M. Freeman (ed.), *Nuclear Medicine Annual 1995*, pp. 1–48. New York: Raven Press Ltd., 1995.
26. Haldemann, A. R., Rösler, H., Barth, A., Waser, B., Geiger, L., Godoy, N., Markwalder, R. V., Seiler, R. W., Sulzer, M., and Reubi, J. C. Somatostatin receptor scintigraphy in patients with CNS tumors: the role of blood brain barrier permeability. *J. Nucl. Med.*, *36*: 403–410, 1995.
27. Jain, R. K. Physiological resistance to the treatment of solid tumors. *In*: B. A. Teicher (ed.), *Drug Resistance in Oncology*, pp. 87–105. New York: Marcel Dekker, Inc., 1993.
28. Bakay, L. The extracellular space in brain tumors. I. Morphological considerations. *Brain*, *93*: 693–698, 1970.
29. Sampson, J. H., Cokgor, I., Akabani, G., Friedman, A., Coleman, E., Friedman, H., McLendon, R., Zhou, X., Bigner, S., Pegram, C., Wikstrand, C., Vick, N., Paleologos, N., Zalutsky, M., and Bigner, D. Radiolabeled anti-tenascin monoclonal antibody in recurrent malignant brain tumors. *Proc. Am. Assoc. Cancer Res.*, *39*: 324–325, 1998.

# Clinical Cancer Research

## Locoregional Regulatory Peptide Receptor Targeting with the Diffusible Somatostatin Analogue <sup>90</sup>Y-Labeled DOTA<sup>0</sup>-d-Phe<sup>1</sup>-Tyr<sup>3</sup>-octreotide (DOTATOC): A Pilot Study in Human Gliomas

Adrian Merlo, Oliver Hausmann, Morten Wasner, et al.

*Clin Cancer Res* 1999;5:1025-1033.

**Updated version** Access the most recent version of this article at:  
<http://clincancerres.aacrjournals.org/content/5/5/1025>

**Cited articles** This article cites 22 articles, 3 of which you can access for free at:  
<http://clincancerres.aacrjournals.org/content/5/5/1025.full#ref-list-1>

**Citing articles** This article has been cited by 12 HighWire-hosted articles. Access the articles at:  
<http://clincancerres.aacrjournals.org/content/5/5/1025.full#related-urls>

**E-mail alerts** [Sign up to receive free email-alerts](#) related to this article or journal.

**Reprints and Subscriptions** To order reprints of this article or to subscribe to the journal, contact the AACR Publications Department at [pubs@aacr.org](mailto:pubs@aacr.org).

**Permissions** To request permission to re-use all or part of this article, use this link  
<http://clincancerres.aacrjournals.org/content/5/5/1025>.  
Click on "Request Permissions" which will take you to the Copyright Clearance Center's (CCC) Rightslink site.